Ref. Ares(2023)180178 - 11/01/2023

Horizon 2020 Programme

STRUMAT-LTO

Research and Innovation Action (RIA)

This project has received funding from the European Union's Horizon 2020 research and innovation programme under grant agreement No 945272

Start date : 2020-09-01 Duration : 48 Months

STRUMAT -LTO

A report on influence of high fluence irradiation on tensile properties of RPV steels and effectiveness of annealing in PWR and VVER 1000 steels

Authors : Mrs. Mathilde LAOT (NRG), Kiki Naziris (NRG), Murthy Kolluri (NRG), Levente Sandor Beres (BZN), Csaba Takacs (BZN), Peter Rozsahegyi (BZN), Szabolcs Szavai (BZN), Milan Brumovsky (UJV), Radim Kopriva (UJV), Milos Kytka (UJV)

STRUMAT-LTO - Contract Number: 945272

Project officer: Panagiotis Manolatos

Document title	A report on influence of high fluence irradiation on tensile properties of RPV steels and effectiveness of annealing in PWR and VVER 1000 steels
Author(s)	Mrs. Mathilde LAOT, Kiki Naziris (NRG), Murthy Kolluri (NRG), Levente Sandor Beres (BZN), Csaba Takacs (BZN), Peter Rozsahegyi (BZN), Szabolcs Szavai (BZN), Milan Brumovsky (UJV), Radim Kopriva (UJV), Milos Kytka (UJV)
Number of pages	35
Document type	Deliverable
Work Package	WP1
Document number	D1.1
Issued by	NRG
Date of completion	2023-01-10 10:24:58
Dissemination level	Public

Summary

This report summarises the results of the tensile testing campaign performed by BZN, NRG and UJV within WP1 of STRUMAT-LTO. Four PWR RPV model steels, eight VVER-1000 RPV base metal model steels and eight VVER-1000 RPV realistic welds were studied. Reference tensile specimens were tested by all 3 partners to obtain the mechanical properties of the materials in as-received unirradiated state. Irradiated specimens were tested by NRG and UJV. The influence of the chemical composition on the extent of irradiation-induced hardening, for neutron fluence values representing 60-80 years of reactor operation, was studied by comparing tensile data of reference and irradiated specimens. Specifically, indications for the existence of a synergetic effect of Ni and Mn in the high-fluence region was investigated. Moreover, some post-irradiation annealing treatments were performed at NRG to study the effectiveness of annealing to retrieve the initial mechanical properties of these steels before irradiation and the influence of chemical composition on the recovery process during annealing. Data is available on the MatDB.

Approval

Date	By
2023-01-10 10:27:19	Dr. Murthy KOLLURI (NRG)
2023-01-10 10:27:51	Dr. Murthy KOLLURI (NRG)

STRUMAT-LTO

Structural Materials for Nuclear Safety and Longevity

Research and Innovation Action

NFRP-2019-2020

Influence of high fluence irradiation on tensile properties of PWR and VVER-1000 RPV model steels and effectiveness of annealing

Deliverable D1.1

Version N°1

Author(s): Mathilde Laot (NRG)

Contributor(s): Kiki Naziris (NRG), Murthy Kolluri (NRG), Levente Sandor Beres (BZN), Csaba Takacs (BZN), Peter Rozsahegyi (BZN), Szabolcs Szavai (BZN), Milan Brumovsky (UJV), Radim Kopriva (UJV), Milos Kytka (UJV)

This project received funding from the Euratom research and training programme 2014-2018 under the grant agreement n°945272.

Disclaimer

Document Information

Grant agreement	945272
Project title	STRUctural MATerials research for safe Long Term Operation of LWR NPPs
Project acronym	STRUMAT-LTO
Project coordinator	Dr. Akos Horvath, MTA-EK
Scientific coordinator	Dr. Murthy Kolluri, NRG
Project duration	1st September 2020 – 31st August 2024 (48 months)
Related work package	WP 1- Embrittlement behaviour of RPV steels at high fluences activities
Related task(s)	Task 1.2 – Tensile Tests
Lead organisation	NRG
Contributing partner(s)	BZN, UJV
Due date	M18
Submission date	26/12/2022
Dissemination level	
NRG reference	24708/23.251387

History

Date	Version	Submitted by	Reviewed by	Comments
18/08/2022	N°1	Mathilde Laot	Kiki Naziris, Milan Brumovsky, Levente Sandor Beres	
06/01/2023	N°2	Mathilde Laot	Murthy Kolluri, Kiki Naziris	

Table of Contents

List of figures

List of tables

Abbreviations and acronyms

Acronym	Description
d_0	Initial specimen diameter (mm)
d_u	Diameter at specimen break (mm)
F_p	Load at yield (kN)
F_m	Maximum load (kN)
F_u	Load at specimen break (kN)
HT	Heat Treatment
L_0	Initial specimen length (mm)
L_u	Length at specimen break (mm)
LTO	Long-Term Operation
NPP	Nuclear Power Plant
PIE	Post-Irradiation Examination
YS	Yield strength
UTS	Ultimate tensile strength
R_u	Fracture stress (MPa)
RPV	Reactor Pressure Vessel
RT	Room temperature
S_0	Initial gauge area (mm^2)
S_u	Gauge area at specimen break (mm^2)
TE	Total Elongation
UE	Uniform Elongation
VVER	Water-cooled water-moderated reactor of Russian design
WP	Work Package
Z	Contraction (%)

Summary

This report summarises the results of the tensile testing campaign performed by BZN, NRG and UJV within WP1 of STRUMAT-LTO. Four PWR RPV model steels, eight VVER-1000 RPV base metal model steels and eight VVER-1000 RPV realistic welds were studied. Reference tensile specimens were tested by all 3 partners to obtain the mechanical properties of the materials in as-received unirradiated state. Irradiated specimens were tested by NRG and UJV. The influence of the chemical composition on the extent of irradiation-induced hardening, for neutron fluence values representing 60-80 years of reactor operation, was studied by comparing tensile data of reference and irradiated specimens. Specifically, indications for the existence of a synergetic effect of Ni and Mn in the high-fluence region was investigated. Moreover, some post-irradiation annealing treatments were performed at NRG to study the effectiveness of annealing to retrieve the initial mechanical properties of these steels before irradiation and the influence of chemical composition on the recovery process during annealing.

Data is available on the MatDB.

Keywords

Long-term operation (LTO); Reactor Pressure Vessel (RPV) embrittlement; LYRA-10 irradiation; thermal annealing; recovery; PWR RPV steels; VVER-1000 steels; Tensile test

1 Introduction

Current nuclear power plants (NPPs) of light-water reactor (LWR) design are considering extension of their operation lifetime or are already operating beyond their original design life. A critical component for ensuring the safe lifetime extension of a LWR beyond its original design life is the reactor pressure vessel (RPV). Exposure of the RPV to fast neutron irradiation during operation causes embrittlement of the RPV with associated changes in mechanical properties (increase in hardening, reduction in ductility). However, surveillance data for RPV steel embrittlement beyond 40 years of operation is limited.

Within the STRUMAT-LTO project, mechanical tests and microstructural analysis on representative RPV model steels (both base and weld metals) irradiated to high fluences are performed to fill this data gap and support Long-term Operation (LTO) of LWRs. STRUMAT-LTO has obtained access to the valuable set of RPV specimens from the LYRA-10 irradiation experiment. LYRA-10 was a joint irradiation experiment carried out by NRG and JRC in the High-Flux-Reactor (HFR), Petten. The RPV specimens in LYRA-10 [[1]] constitute both RPV base and weld model alloys resembling western type PWR and VVER-1000 RPVs with systematic variations in the content of Ni and Mn and to a smaller extent Si . The specimens were irradiated to high fluences resembling reactor operation times of 60-80 years at temperatures typical for PWR / VVER operation, i.e., 286 °C. For each type of RPV model steel, a variety of specimens constituting tensile, Charpy, half-thick Charpy, miniature Charpy (KLST type), and small slices for miniature and microstructural investigations are available. Post-irradiation examination (PIE) is performed within this project to investigate the synergetic effects of Ni and Mn on RPV steels embrittlement at high fluences. In addition, as the current knowledge and data on recovery annealing treatment and re-irradiation behaviour of low-Cu and high-Ni RPV steels is limited, the influence of thermal annealing on the recovery of mechanical properties of highly irradiated low-Cu RPV steels will be investigated.

This report presents the results from the tensile tests of 8 VVER-1000 RPV base metal (BM) model steels (grades A – H), 8 VVER-1000 RPV realistic welds (grades A – H) and 4 PWR RPV BM model steels (grades K – N) performed by BZN, NRG and UJV. The tensile tests are performed on unirradiated (reference), irradiated (in LYRA-10) and post irradiation annealed specimens. Influence of chemical composition, specifically Ni, Mn and Si, on irradiation hardening and ductility is studied. Effectiveness of post-irradiation annealing treatment, performed at two different annealing temperatures, to recover the initial mechanical properties (tensile properties) before irradiation is investigated for the different RPV model steels and realistic welds.

2 Experimental

2.1 Materials

In this work, eight different VVER-1000 RPV BM model steels referred hereafter as model steels grade A, B, C, D, E, F, G and H are studied. Their chemical composition is given in Table 1. Besides, eight VVER-1000 RPV realistic welds referred hereafter as realistic weld grade A, B, C, D, E, F, G and H are studied and their chemical composition is given in Table 2.

Steel type	Steel Id.	C	Si	Mn	Cr	Ni	Mo	V	Cu	S	P
VVER-1000 RPV BM model steels	A	0.11	0.28	0.43	2.22	<0.02	0.71	0.1	0.09	0.008	0.01
	B	0.11	0.26	0.38	2.19	0.99	0.7	0.1	0.1	0.008	0.01
	C	0.12	0.24	0.38	2.13	2	0.69	0.1	0.1	0.008	0.01
	D	0.11	0.23	0.83	2.13	2	0.68	0.1	0.09	0.008	0.009
	E	0.12	0.33	0.77	2.16	1.02	0.7	0.1	0.1	0.008	0.009
	F	0.12	0.33	1.37	2.15	1.02	0.7	0.1	0.1	0.008	0.01
	G	0.11	0.32	1.36	2.06	1.99	0.69	0.1	0.1	0.008	0.009
	H	0.12	0.51	1.31	2.07	2	0.69	0.1	0.1	0.008	0.01

Table 1. Chemical composition of the eight VVER-1000 RPV BM model steels (in mass %)

Steel type	Steel Id.	C	Si	Mn	Cr	Ni	Mo	V	Cu	S	P	Co	As	Sn
VVER-1000 RPV realistic welds (I)	A	0.07	0.18	0.57	2.07	1.3	0.59	0.09	0.06	0.007	0.011	0.02	0.004	0.005
	B	0.06	0.31	0.56	2.04	1.59	0.6	0.09	0.06	0.009	0.007	0.02	0.004	0.005
	E	0.05	0.3	0.89	2	1.94	0.57	0.09	0.06	0.009	0.006	0.02	0.004	0.004
	H	0.06	0.32	1.08	1.98	1.89	0.58	0.09	0.06	0.001	0.007	0.02	0.004	0.005
VVER-1000 RPV realistic welds (II)	C	0.05	0.32	0.6	1.95	1.87	0.58	0.08	0.06	0.01	0.007	0.02	0.004	0.005
	D	0.06	0.29	0.72	2.01	1.57	0.59	0.09	0.06	0.009	0.006	0.02	0.004	0.004
	F	0.06	0.29	1.07	2.04	1.26	0.58	0.09	0.06	0.009	0.006	0.02	0.004	0.004
	G	0.06	0.3	1.07	2.04	1.57	0.59	0.09	0.06	0.001	0.007	0.02	0.004	0.005

Table 2. Chemical composition of the eight VVER-1000 RPV realistic welds (in mass %)

In addition to the above mentioned VVER-1000 BM and realistic weld RPV steels, four different PWR RPV BM model steels, referred hereafter as model steels grade K, L, M and N, are studied. Their chemical composition is given in Table 3.

Steel Type	Steel Id.	C	Si	Mn	Cr	Ni	Mo	V	Cu	S	P
PWR RPV BM model steels	K	0.17	0.35	0.78	0.10	0.58	0.64	-	0.07	0.005	0.009
	L	0.18	0.35	0.77	0.08	0.96	0.63	-	0.05	0.005	0.010
	M	0.16	0.37	0.74	0.09	1.90	0.61	-	0.05	0.005	0.010
	N	0.16	0.33	1.27	0.07	1.97	0.63	-	0.06	0.005	0.010

Table 3. Chemical composition of the four PWR BM model steels (in mass %)

The variation in Ni, Mn and Si content allowed to investigate their individual and synergetic effects on the embrittlement of VVER-1000 RPV BM and realistic weld steels and PWR RPV BM model steels at high fluences. Moreover, the influence of composition on the effectiveness of annealing treatments is studied.

It should be noted that the chemical composition of the model steels (VVER-1000 and PWR) and realistic welds (VVER-1000) used for this research purposefully deviate from specifications of VVER-1000 and PWR RPV steels to be able to study the effect of Ni, Mn and Si. The base composition is kept constant for all grades while the contents of Ni, Mn and Si are varied.

2.2 Irradiation

Irradiation was carried out jointly by NRG and JRC in the High-Flux Reactor (HFR) in Petten. Irradiation lasted for 16 HFR cycles (~467 full power days at nominal reactor power level of 45 MW) to achieve a nominal fast neutron fluence (E > 1 MeV) of 1.11 x 10^{20} n.cm^{-2} at an average temperature of 286 °C. The fluence received per specimen is given in Appendix A.

2.3 Post-irradiation annealing treatments

At NRG, post-irradiation annealing treatments at different temperatures on the above RPV BM model steels and realistic welds were performed to investigate to what extent their original mechanical properties could be recovered. In case of the 8 VVER 1000 BM models steels, selected samples from each grade were annealed in air at 340°C for 150 hours and at 475°C for 100 hours. For 4 realistic welds, selected samples were annealed in air at 418°C for 150 hours and at 475°C for 100 hours. For the 4 PWR BM model steels, the samples were annealed in air at 450 °C for 40 hours. For all different annealing treatments, furnace cooling was applied.

2.4 Test methods

Tensile tests on reference (unirradiated) and irradiated samples were performed by BZN, NRG and UJV. Table 4 Summarises the tensile tests performed by the three organisations.

Partner	Steel type	Grades	Un-/irradiated	Test Temperature
BZN	VVER-1000 RPV BM model steels	A – H	Unirradiated	RT
	PWR RPV BM model steels	K, L, M, N	Unirradiated	RT
NRG	VVER-1000 RPV BM model steels	A – H	Unirradiated	RT/300 °C
	VVER-1000 RPV BM model steels	A – H	Irradiated	RT
	VVER-1000 RPV realistic welds	A, B, E, H	Unirradiated	RT/300 °C
	VVER-1000 RPV realistic welds	A, B, E, H	Irradiated	RT
	PWR RPV BM model steels	K, L, M, N	Unirradiated	RT/100 °C
	PWR RPV BM model steels	K, L, M, N	Irradiated	RT
UJV	VVER-1000 RPV realistic welds	C, D, F, G	Unirradiated	RT/300 °C
	VVER-1000 RPV realistic welds	C, D, F, G	Irradiated	RT/300 °C

Table 4. Overview of tensile tests of the three partners

Table 5 shows the equipment, standards and test condition used by the three organisations for their tensile tests.

	BZN	NRG	UJV
Testing Equipment	Instron 8874 Biaxial universal servo hydraulic material testing equipment	Instron 1362 Servo-mechanical material testing equipment	Instron 8802 Servo hydraulic material testing equipment
Extensometer	Epsilon axial extensometer (GL: 6 mm, TR: 1,2 mm)	-	-
Standard	ISO 6892-1	ASTM E8M / ASTM E21	CSN EN ISO 6892-1 / CSN EN ISO 6892-2
Test speed	0,5 mm/min	0,7 mm/min	0,8 mm/min
Test temperature	Room temperature	Room temperature / 100 °C / 300 °C	Room temperature / 300 °C

Table 5 Summary of test conditions at BZN, NRG and UJV

Two types of tensile specimens were used. For the realistic welds tensile specimens with a diameter of 3 mm and a gauge length of 30 mm were used, as shown in Figure 1. Tensile specimens of the RPV BM model steels have a diameter of 3 mm and a gauge length of 22 mm, as shown in Figure 2.Figure 2 Geometry of tensile specimens VVER-1000 and PWR RPV model steels

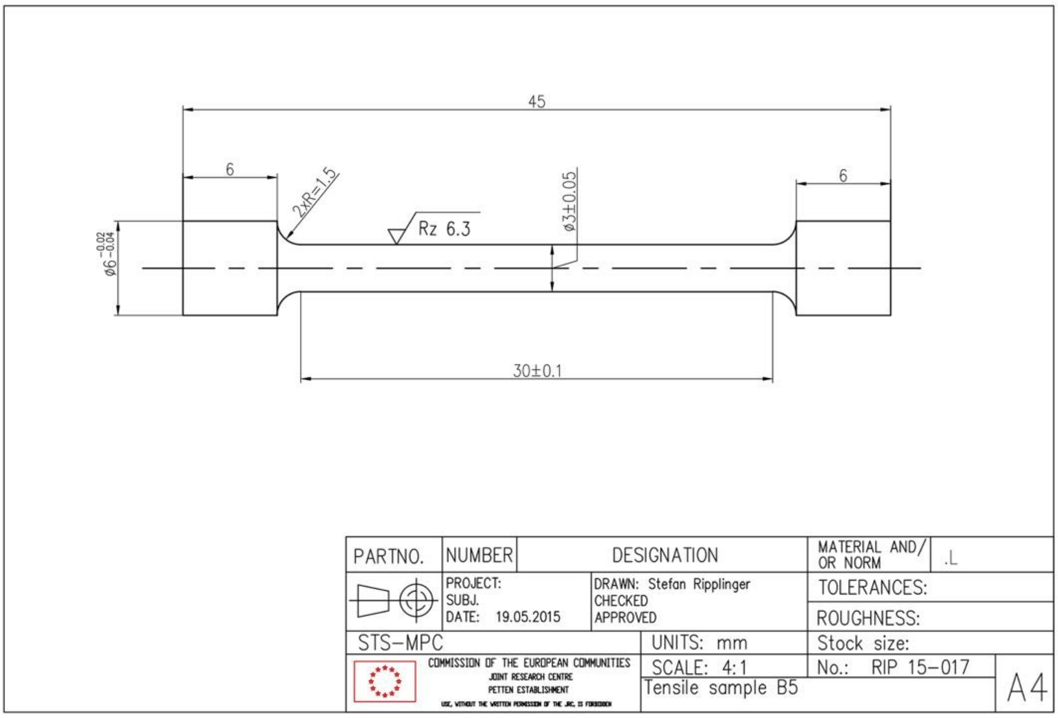

Figure 1 Geometry of tensile specimens VVER-1000 RPV realistic welds

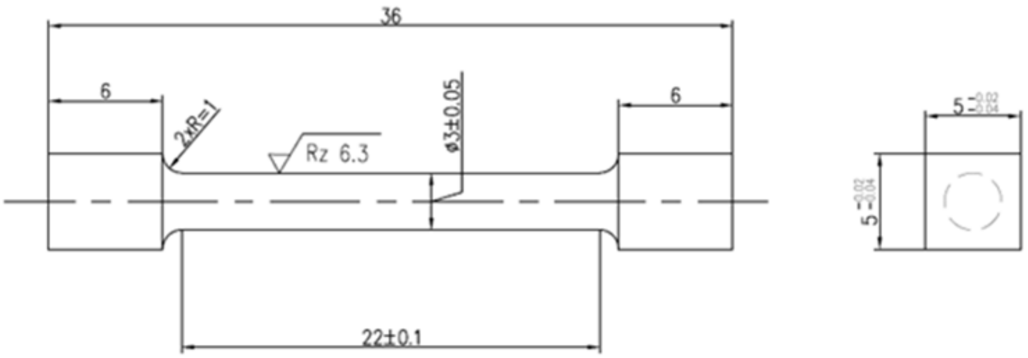

Figure 2 Geometry of tensile specimens VVER-1000 and PWR RPV model steels

3 Results and discussion

3.1 Influence of chemical composition

3.1.1 VVER-1000 RPV base metal model steels

The combined effect of Ni and Mn on irradiation hardening of all the 8 model steels is shown in Figure 3. Irradiation hardening increases with rising combined content of Ni and Mn.

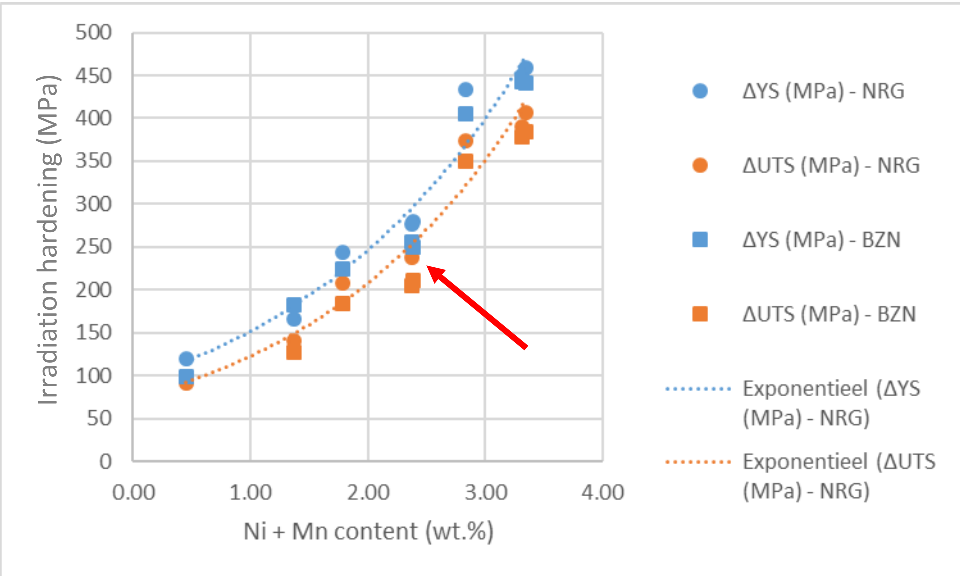

Figure 3 Effect of Ni and Mn content on hardening of VVER-1000 RPV BM model steels

Also it has been observed that model steel grades with similar combined Ni+Mn content but different individual contents in Ni and Mn show similar hardening increases. Both model steel grades C and F (indicated by an arrow in Figure 3) have approximately the same combined Ni+Mn content (2,38 % for grade C and 2,39 % for grade F) but different individual contents in Ni (2 % for grade C and 1.02 % for grade F) and Mn (0.38 % for grade C and 1.37 % for grade F), and they showed similar hardening increases: ΔYS_C = 277 MPa and ΔYS_F = 279 MPa, ΔUTS_C = 238 MPa and ΔUTS_F = 246 MPa. Similar behaviour was observed between grades G and H (Ni+Mn content of 3.31-3.35%).

Model steels D, G and H, all containing a combined Ni+Mn content ≥ 2.83%, showed a steep rise in irradiation hardening compared to the rest of the steels. These three model steels have a Ni content of ~ 2% such as grade C. However, grade C has a lower Mn content compared to grades D, G and H. The observed higher increase in irradiation hardening suggests a synergetic effect of Ni and Mn. These observed results are similar to the four PWR BM model steels that show evidence of a synergetic effect between Ni and Mn when the combined Ni+Mn content is ≥ 2.90% [[1]]. An extensive investigation on the microstructure of these grades is required to understand in detail the root cause (i.e. cluster formation) behind the observed increases in hardening.

Moreover as seen on Figure 3, significant differences in strength are observed for different samples from the same steel grade. Additional tests were performed by NRG and BZN to understand these differences. Some remaining tensile specimens of grade A, F and G were tested by both NRG and BZN. The results of these additional tensile tests showed discrepancies as well. Figure 4 shows the comparison between the specimens tested in 2022/2021 and the additional tests performed in September 2022. Hardness tests (HV10) were then performed, as well as optical microscopy to determine whether inhomogeneity in microstructure could be the reason of the observed discrepancies. Samples from the broken pieces of 3 tensile specimens from grade A were used for the tests. Grade A was selected since it showed the highest discrepancy in strength between specimens. The results are summarized in Table 1. It can be seen that differences in hardness are observed between samples from the two heads of the tensile specimens, and between the different tensile specimens. A difference of 10 – 20 HV is observed which could mean a difference of 37 to 63 MPa in tensile strength as calculated following ASTM A370 [2]. The results suggest that inhomogeneity in the microstructure of the tensile specimens and could explain the observed discrepancies in yield and ultimate tensile strength. However no significant difference in microstructure is observed with optical microcopy (at magnification of 250 and 500). In WP3, the initial microstructure was studied and model steel grade A shows an inhomogeneous bainitic microstructure. The hardness measurements performed in WP3 on 1 sample show differences in values depending on the orientation [3]. The findings are in accordance with the additional measurements performed in WP1.

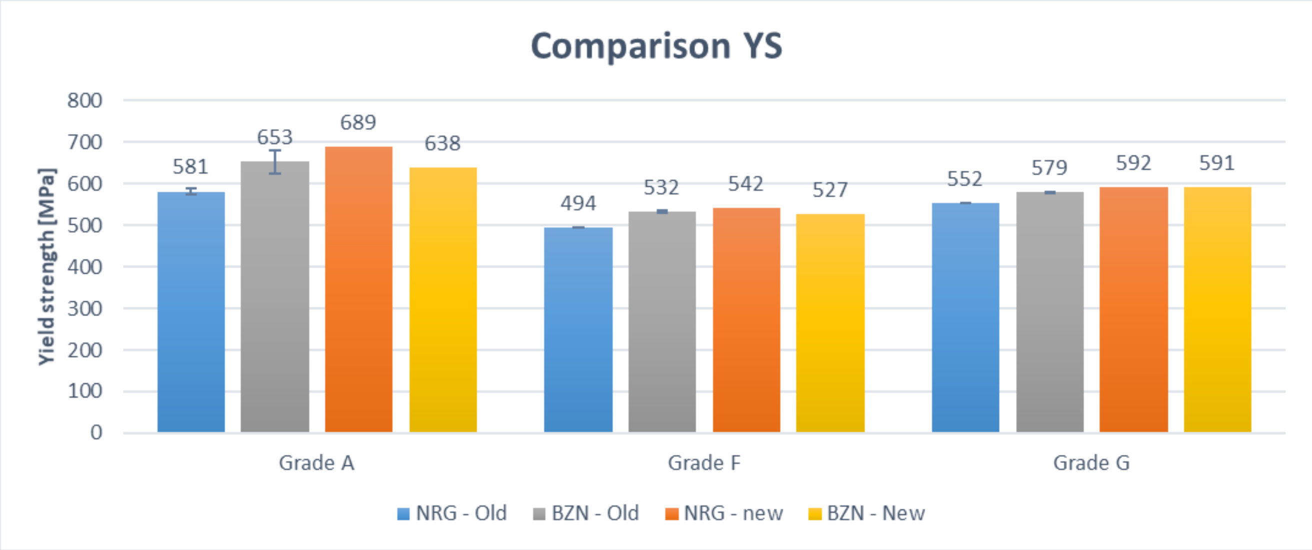

Figure 4 Comparison yield strength between tensile specimens of grade A, F and G. Old refers to the average of the yield strength measured for 2 (NRG) and 3 (BZN) tensile specimens in 2020/2021 and new refers to the yield strength of 1 tensile specimen tested in September 2022

Table 1 Hardness tests on VVER model steels grade A

	Spec. Number	Cross section				Longitudinal cross section			
		Specimen head I		**Specimen head II**		Specimen head I		**Specimen head II**	
		HV10	HV10_avg	**HV10**	**HV10_avg**	HV10	HV10_avg	**HV10**	**HV10_avg**
BZN	AA4-1 old	263 273 267	268	**259** **254** **255**	**256**	268 278 275	274	**243** **265** **250**	**253**
	AA5-2 new	269 263 267	266	**279** **286** **285**	**283**	263 267 265	265	**285** **288** **275**	**283**
NRG	AA5-1 new	278 282 270	276	**279** **271** **267**	**272**	284 288 285	286	**266** **265** **271**	**267**

3.1.2 VVER-1000 RPV realistic welds

Also for the realistic welds an increase in hardening is observed with rising combined Ni+Mn content, as shown in Figure 4, but the increase in work hardening does not follow such a clear trend as for the VVER-1000 RPV BM model steels in Figure 3.

Grades A and B have similar hardening increases (ΔUTS_A= 207 MPa and ΔUTS_B= 200 MPa, ΔYS_A= 248 MPa and ΔYS_B= 245 MPa). For grades with a combined Ni+Mn content between 2.29% and 2.83% (grades C, D, E, F, G), a gradual increase of irradiation hardening has been observed. No clear trend was observed for an increase in Ni-content only or Mn-content only.

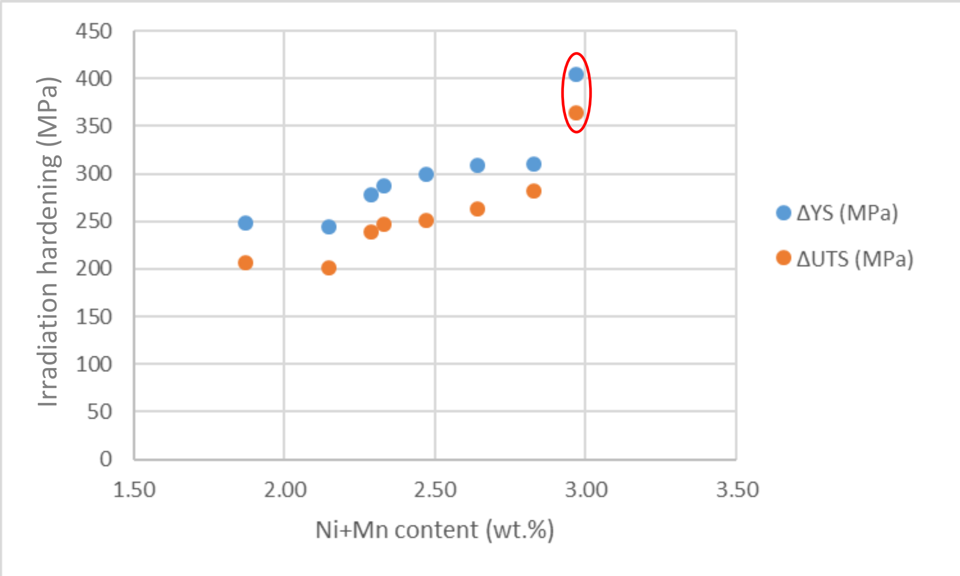

Figure 5 Effect of Ni + Mn content on the hardening of VVER-1000 RPV realistic welds

Realistic weld grade H, with high individual content of Ni and Mn each and consequently a high combined Ni+Mn content (2.97%), showed a steep rise in irradiation hardening compared to rest of the welds. It is interesting to note that this steep rise is observed only in grade H. The combined Ni+Mn content is close to the threshold value (~2.90%) at which a possible synergetic effect between Ni and Mn is expected [4] resulting in severe irradiation hardening.

3.1.3 PWR RPV base metal model steels

The results of the tensile tests on the four PWR RPV BM model steels, unirradiated and irradiated, have been published before [4]. A summary of the results is given below.

Mechanical properties (YS, UTS, %UE and %TE) of all four PWR RPV BM model steels in reference and irradiated conditions are shown in Figure 6. It can be seen that strength and ductility properties in the reference condition were quite similar for all four model steels as expected. Significant differences in the strength properties after irradiation have been observed between different model steels while the observed changes in ductility properties are minimal.

The difference of irradiation hardening between the four PWR RPV BM model steels illustrates the influence of effect of Ni and Mn. An increase in Ni-content from 0.58% in model steel K to 0.96% in model steel L has resulted in a negligible difference in irradiation induced hardening. However, an increase in Ni content from 0.96% to 1.90%, at the same Mn content (0.74 – 0.77

%), has resulted in a significant increase in irradiation induced hardening in model steel M when compared to model steel L. This indicates that the role of Ni for irradiation hardening becomes increasingly significant in RPV steels with higher Ni content. Lastly, the steep increase in irradiation hardening observed for model steel N (1.27% of Mn) compared to model steel M (0.74% of Mn) indicates the adverse role of Mn in irradiation hardening of RPV steels of high Ni-content at high neutron fluences.

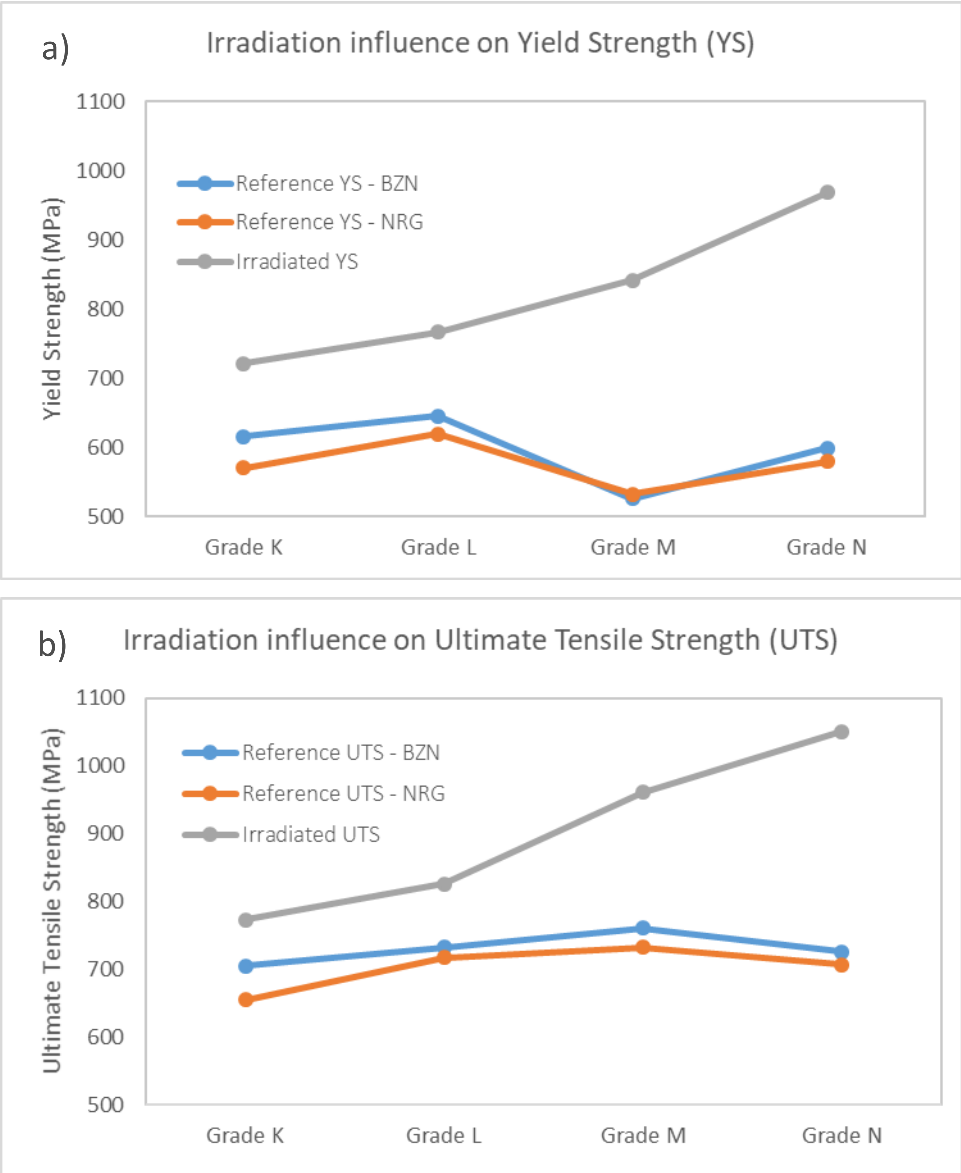

Figure 6 Comparison of a) YS and b) UTS properties of four PWR RPV BM model steels in reference and irradiated conditions.

3.2 Influence of thermal annealing treatments

Only NRG performed post-irradiation annealing treatments. Their effectiveness in recovering tensile properties of the initial unirradiated state for various model steels is discussed below.

3.2.1 VVER-1000 RPV base metal model steels

The effect of the annealing treatments on the yield strength and on the ultimate tensile strength for all 8 model steel grades is shown in Figure 7 and in Figure 9. Annealing at 340°C for 150 hours has not given any recovery in tensile properties of all the model steel grades. Yield strength and ultimate tensile strength after annealing are pretty much the same as for the irradiated state for all 8 model steels. In contrast after annealing at 475 °C for 100 hours an almost full (~99%) recovery of tensile properties is achieved for all model steel grades. The recovery of strength properties after annealing at 475 ºC indicates that no, or only insignificant, thermodynamically stable phases are formed due to irradiation to high neutron fluences.

Variations in Ni-, Mn- and Si-content of the model steels has no impact on the effectiveness of annealing treatment. Full recovery in tensile properties is achieved for all 8 model steels irrespective of their Ni, Mn and Si contents. Annealing temperature is the decisive factor.

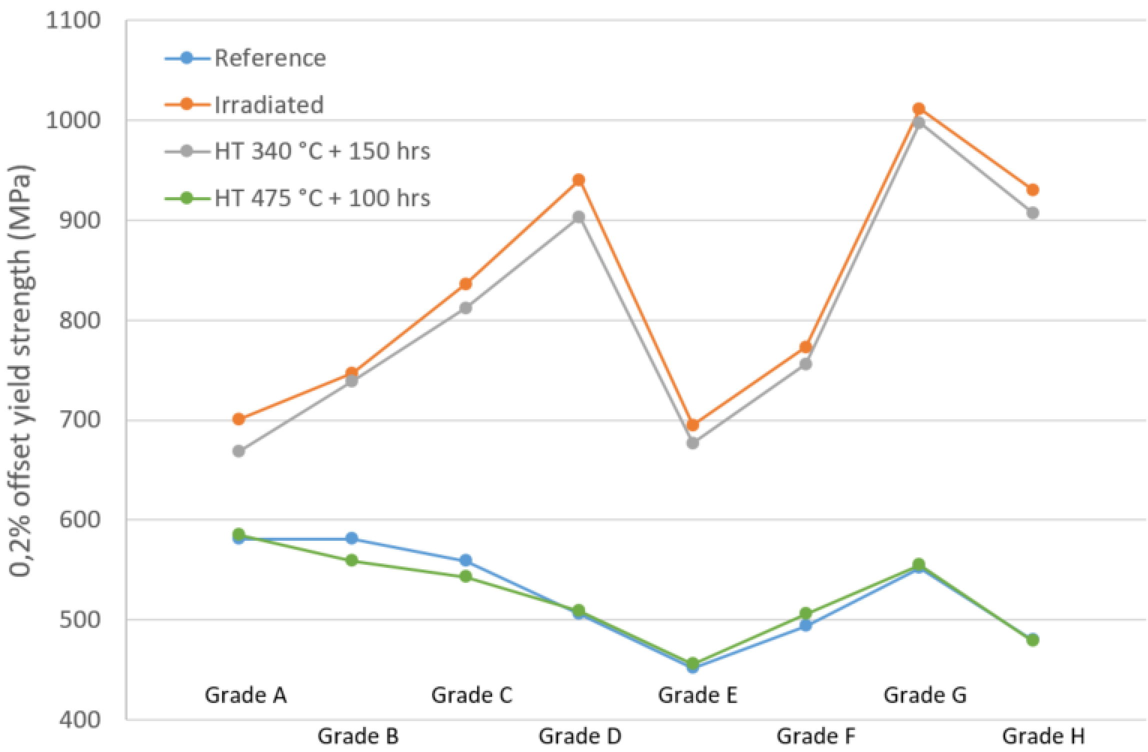

Figure 7 Influence of annealing on 0.2% offset yield strength of VVER-1000 BM model steels

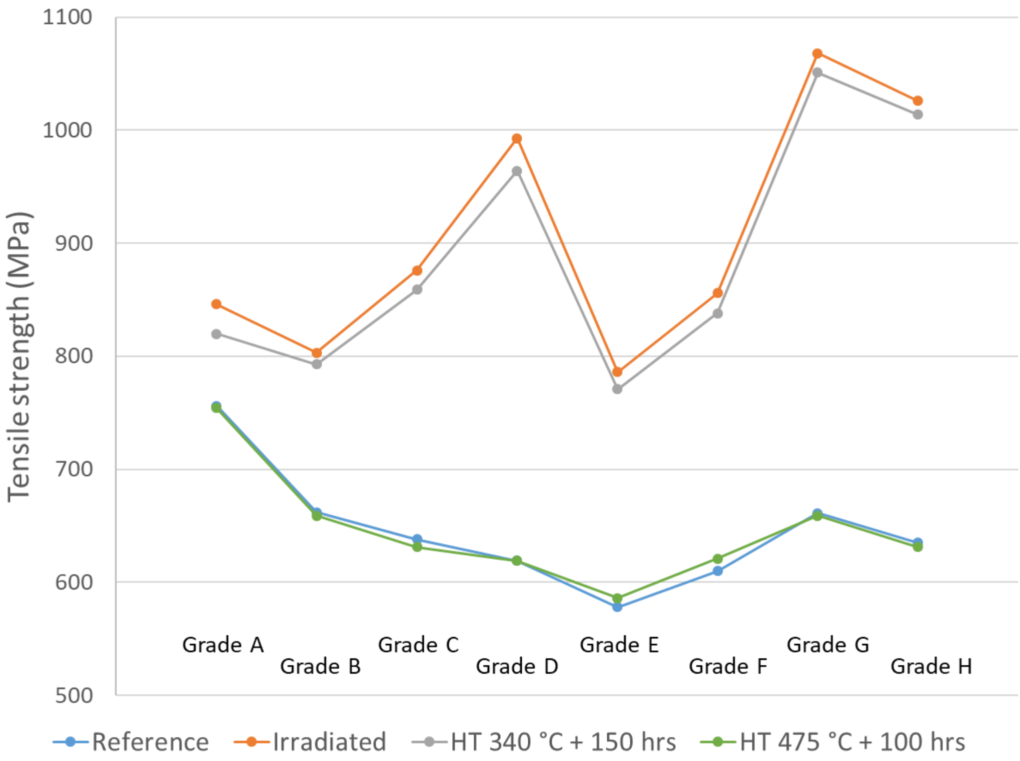

Figure 9 Influence of annealing on tensile strength of VVER-1000 BM model steels

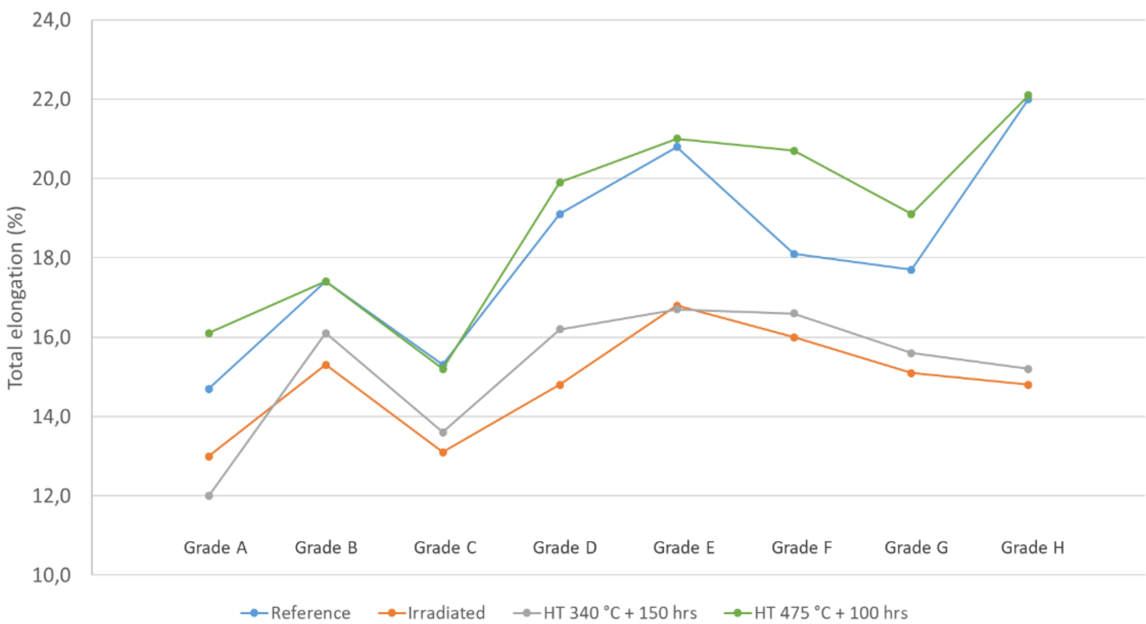

Figure 8 Influence of annealing on total elongation of VVER-1000 BM model steels

Full recovery of ductility (even improvement compared to unirradiated state) is observed after annealing at 475 °C for all model steel grades, as shown in Figure 8. Annealing at 340 °C has not resulted in any significant recovery of ductility for the different model steel grades. No clear effect of irradiation and annealing are observed on uniform plastic strain.

3.2.2 VVER-1000 RPV realistic welds

The effect of annealing on the recovery of tensile properties of the four realistic welds A, B, E and H is shown in Figure 10 and Figure 11. Almost full recovery of yield strength and tensile strength were achieved after both annealing treatments for welds A, B and E.

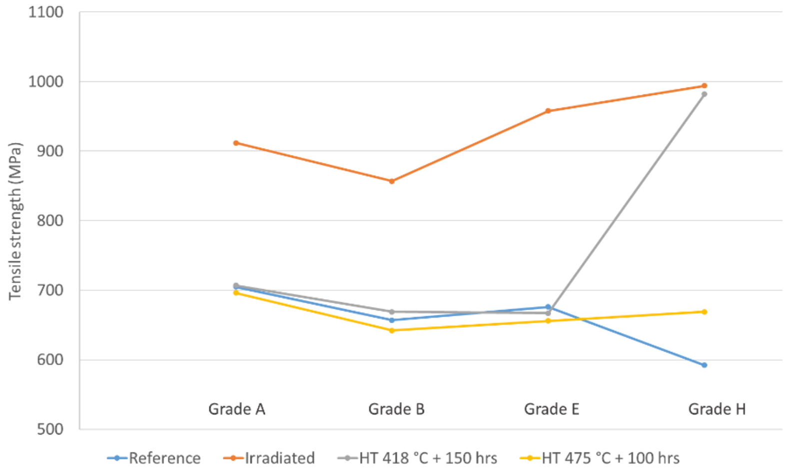

Figure 10 Influence of annealing on tensile strength on VVER-1000 realistic welds

For the realistic weld grade H, only annealing at higher temperature (475°C for 100 hours) resulted in significant (~87%) but not full recovery of tensile properties. Full recovery could probably be achieved either by prolonging the annealing time or slightly increasing the annealing temperature for this realistic weld grade H. The reason for incomplete recovery is topic of future study. Annealing at 418°C has not resulted in any recovery of tensile properties of realistic weld H. It has a higher Mn-content in combination with high Ni-content, with a combined Ni+Mn content of 2.97%, which is significantly higher than the other three realistic welds investigated here. The results from the PWR RPV BM model steels have shown evidence of synergetic effect between Ni and Mn if the combined Ni+Mn content is ≥ 2.90% [4]. This high combined Ni+Mn content could explain the severe irradiation hardening and lower effectiveness of annealing treatments observed in realistic weld grade H. In addition the realistic weld grade H specimens received slightly higher fluence compared to the realistic weld grade E which also have high combined Ni+Mn content (= 2.83%).

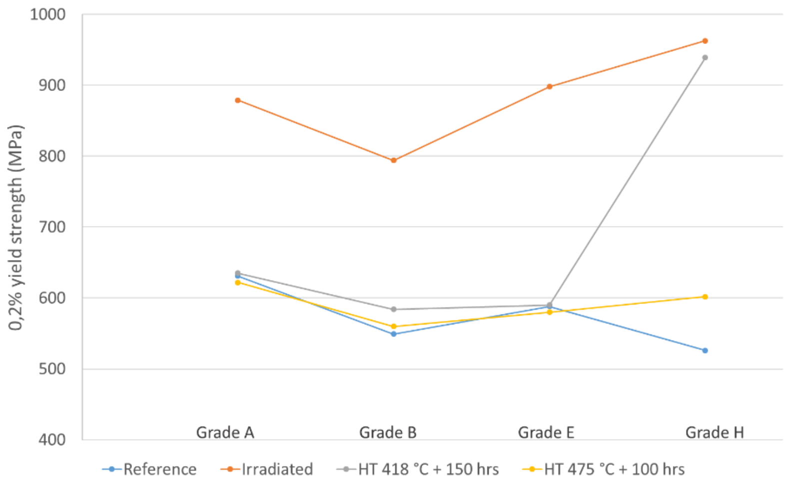

Figure 11 Influence of annealing on 0.2% yield strength on VVER-1000 realistic welds

No significant effect of the annealing treatments on the uniform plastic strain and on the total elongation was observed. Neither the higher annealing temperature nor the chemical composition of the realistic welds resulted in a significant effect.

3.2.3 PWR RPV base model steels

From Figure 12 it can be seen that the annealing treatment led to a significant recovery of tensile properties for all four model steels. The relative recovery of the yield strength (YS) is slightly lower than the recovery of the ultimate tensile strength (UTS), except for grade M, which shows a significant difference between YS and UTS recovery. The recovery of YS for grades K, L, and M are similar while grade N, with a higher content of Mn (1.27 wt.% compared to 0.74–0.78 wt.% for K, L and M), shows a higher recovery of YS. Model steels with high Ni content (grades M and N) show a higher recovery of UTS than with lower Ni content (grades K and L). Recovery of uniform elongation and total elongation is found to be negligible. Only a slight change in ductility was observed after irradiation, and after annealing the elongation values (%TE and %UE) are close to irradiated values. Only Grade N with its higher Mn content shows a slight recovery of its total elongation.

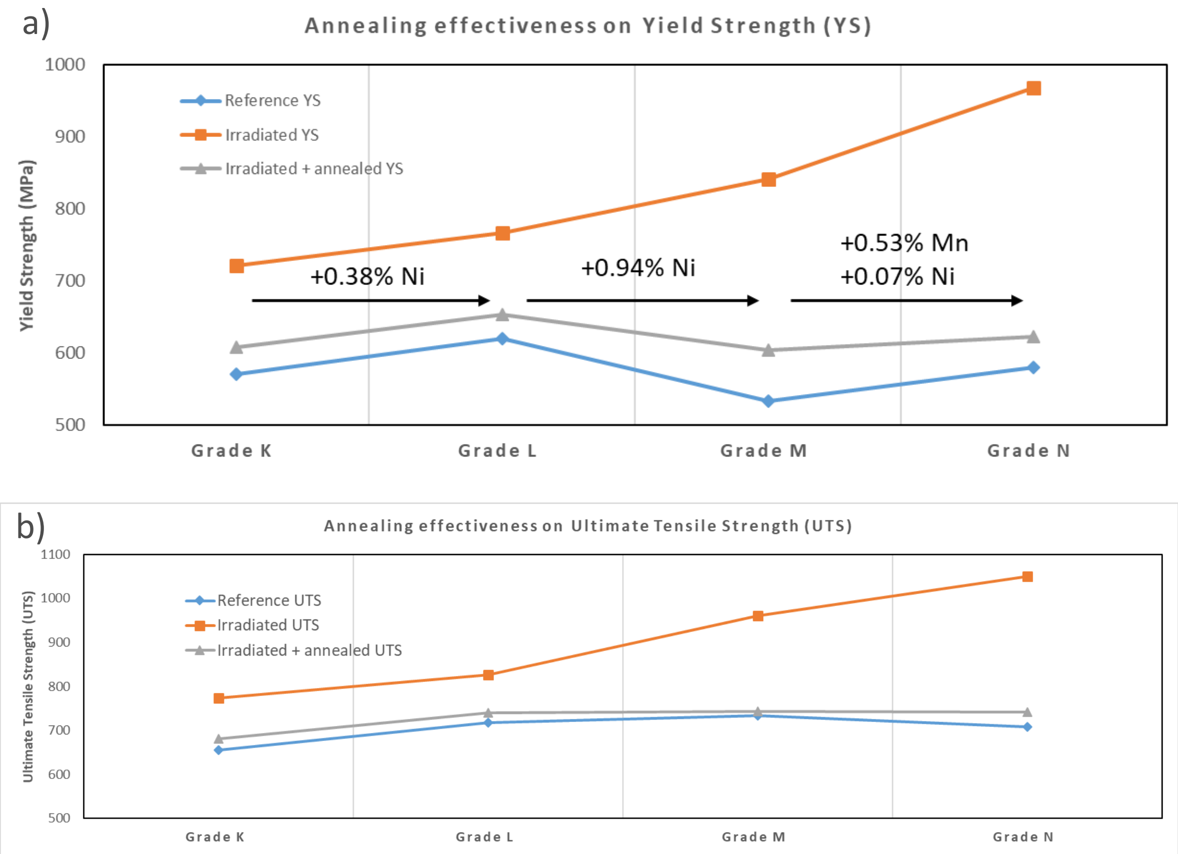

Figure 12 Comparison of a) YS and b) UTS properties of the 4 PWR RPV BM model steels in reference, irradiated and irradiated-annealed conditions.

All four investigated RPV BM model steels show significant recovery of their strength properties after recovery annealing treatment. This recovery is believed to be related to the (partial) dissolution of the radiation-induced clusters and the annihilation of matrix defects. The dissolution of the radiation-induced Ni-Mn-Si-rich precipitates in low-Cu RPV steels upon annealing has been already demonstrated in various studies (e.g., [5][6][7]).

The fluence values that the specimens in this study received resemble more than 60 years of reactor operation (nominal fast fluence values of 1.05–1.22 × 10^{20} cm^{-2}). The significant recovery of the strength properties of all examined model steels after only 40 h of annealing at the relatively modest temperature of 450 °C indicates almost full dissolution of irradiation-induced Ni-Mn-Si-rich clusters and matrix defects. Moreover, the recovery of strength properties indicates that no, or only insignificant, thermodynamically stable phases are formed due to irradiation to high neutron fluences. It should be noted that slight differences exist in the level of recovery of YS and UTS between the four model steel types. The lower recovery in YS of grade M could indicate a delay in the yield point phenomenon, likely due to the presence of some residual irradiation defects offering resistance to the dislocation motion. The residual hardening still present in all four model steel types after annealing is most likely related to the chosen annealing treatment. An annealing temperature above 450°C (e.g. 475°C as for the VVER-1000 RPV BM model steels) and a longer annealing period (e.g. 150h instead of 40 h) could be sufficient to fully dissolve all the Ni-Mn-Si-rich clusters.

The results of the tensile tests on the four PWR RPV BM model steels K, L, M and N for all states (unirradiated, irradiated, irradiated and subsequent annealing) have been published before in [8] and in [9][9][9].

In-depth results (individual specimen data) of all the tensile tests performed by the three involved STRUMAT-LTO project partners are summarized in Appendix B.

CONCLUSION

The influence of variation in chemical composition, most notably contents of Ni, Mnand Si, on irradiation hardening and embrittlement of different VVER-1000 and PWR RPV BM model steels and VVER-1000 realistic welds was studied in this report. A strong correlation was found between combined Ni+Mn content and the extent of irradiation hardening. For any given steel the observed increase in irradiation hardening is directly correlated to the combined Ni+Mn content irrespective of the individual content of Ni and Mn. Severe hardening was observed in all the model steels and realistic welds containing a combined Ni+Mn content ≥ 2.83%, which indicates a synergetic effect between Ni and Mn. Annealing of irradiated specimens proved to be effective in recovering the initial tensile properties at unirradiated state of the various steel grades, depending upon the annealing conditions (mainly temperature). Annealing at 475°C resulted in an almost full recovery of the tensile properties before irradiation for all model steels. For VVER-1000 RPV BM model steels, the chemical composition of the steel grades have not shown any impact on the recovery results. Initial tensile properties could be fully restored for all VVER-1000 RPV BM model steels. Only in case of one of the VVER-1000 RPV realistic welds – Grade H – initial tensile properties could not be fully recovered by annealing at 475°C and 100h. This could be explained by the extremely high combined Ni+Mn content leading to a very high level of hardening due to irradiation. Nevertheless a significant recovery in tensile properties of 87% has been achieved for realistic weld H. Particular attention will be given to this weld steel during microstructural analyses. For PWR RPV steels, some influence of the chemical composition on the recovery process during annealing was observed. Model steels with high Ni and Mn content showed slightly higher recovery than steels with lower Ni and Mn content. Moreover the recovery of strength properties indicates that no, or only insignificant, thermodynamically stable phases are formed due to irradiation to high neutron fluences.

Bibliography

[1] A. Ballesteros, R. Ahlstrand, C. Bruynooghe, U. v. Estrorff en L. Debarberis, „The role of pressure vessel embrittlement in the long term operation of nuclear power plants," *Nuclear Engineering and Design*, 2012, vol. 243, pp. 63-68.

[2] ASTM A 370, Standard Test Methods and Definitions for Mechanical Testing of Steel Products, October 2003.

[3] Elvira Oñorbe, D.3.1. Test matrix and characterization on the initial microstructures, STRUMAT-LTO report, 22 August 2021.

[4] M. Kolluri, P. ten Pierick, T. Bakker, B. T. Straathof, A. J. Magielsen, Z. Szaraz, E. D'Agata, C. Ohms and O. Martin. Influence of Ni-Mn contents on the embrittlement of PWR RPV model steels irradiated to high fluences relevant for LTO beyond 60 years. *J. Nucl. Mater.*, 2021, 553.

[5] Yabuuchi, K.; Saito, M.; Kasada, R.; Kimura, A. Neutron irradiation hardening and microstructure changes in Fe–Mn binary alloys. *J. Nucl. Mater.* 2011, *414*, 498–502.

[6] Gillemot, F. Review on Steel Enhancement for Nuclear RPVs. *Metals* 2021, *11*, 2008.

[7] Gurovich, B.; Kuleshova, E.; Shtrombakh, Y.; Fedotova, S.; Zabusov, O.; Prikhodko, K.; Zhurko, D. Evolution of weld metals nanostructure and properties under irradiation and recovery annealing of VVER-type reactors. *J. Nucl. Mater.* 2013, *434*, 72–84, 2013.

[8] Laot, M.; Naziris, K.; Bakker, T.; D'Agata, E.; Martin, O. & Kolluri, M. Effectiveness of Thermal Annealing in Recovery of Tensile Properties of Compositionally Tailored PWR Model Steels Irradiated in LYRA-10. *Metals* 2022, 12, 904, https://doi.org/10.3390/ met12060904.

[9] M. Laot, M. Kolluri, STRUMAT-LTO : Results of tensile and annealing tests performed at NRG, NRG note, 24708/21.229503.

[10] E. D'Agata, B. Acosta, LYRA-304/10 Irradiation Report, JRC Technical Reports, 2018.

Appendix A

Fluence per specimen

Specimen ID.	E>1 MeV [n/m^{-2}]	E>0.5MeV [n/m^{-2}]	Avg. Temp [°C]
AA 11	8.044E+23	1.403E+24	266.1
AA 12	8.132E+23	1.417E+24	266.1
AA 13	8.243E+23	1.436E+24	266.1
AA 21	8.365E+23	1.457E+24	266.1
AA 22	8.497E+23	1.479E+24	266.1
AA 23	8.644E+23	1.505E+24	266.1
BA 11	8.808E+23	1.533E+24	266.1
BA 12	8.985E+23	1.564E+24	266.1
BA 13	9.141E+23	1.590E+24	266.1
BA 21	9.643E+23	1.689E+24	277.7
BA 22	9.737E+23	1.705E+24	277.7
BA 23	9.855E+23	1.726E+24	277.7
CA 11	9.985E+23	1.749E+24	277.7
CA 12	1.013E+24	1.773E+24	277.7
CA 13	1.028E+24	1.801E+24	277.7
CA 21	1.046E+24	1.831E+24	277.7
CA 22	1.065E+24	1.865E+24	277.7
CA 23	1.081E+24	1.894E+24	277.7
DA 11	1.078E+24	1.890E+24	285.0
DA 12	1.089E+24	1.908E+24	285.0
DA 13	1.102E+24	1.931E+24	285.0
DA 21	1.116E+24	1.956E+24	285.0
DA 22	1.132E+24	1.983E+24	285.0
DA 23	1.149E+24	2.014E+24	285.0
EA 11	1.169E+24	2.048E+24	285.0
EA 12	1.189E+24	2.085E+24	285.0
EA 13	1.208E+24	2.117E+24	285.0
EA 21	1.136E+24	1.990E+24	288.0
EA 22	1.147E+24	2.009E+24	288.0
EA 23	1.161E+24	2.034E+24	288.0
FA 11	1.176E+24	2.060E+24	288.0
FA 12	1.193E+24	2.090E+24	288.0
FA 13	1.211E+24	2.122E+24	288.0
FA 21	1.232E+24	2.158E+24	288.0
FA 22	1.254E+24	2.197E+24	288.0
FA 23	1.273E+24	2.231E+24	288.0
GA 11	1.137E+24	1.992E+24	289.0
GA 12	1.148E+24	2.011E+24	289.0
GA 13	1.162E+24	2.036E+24	289.0
GA 21	1.177E+24	2.062E+24	289.0
GA 22	1.194E+24	2.091E+24	289.0
GA 23	1.212E+24	2.123E+24	289.0
HA 11	1.233E+24	2.159E+24	289.0
HA 12	1.255E+24	2.198E+24	289.0
HA 13	1.274E+24	2.233E+24	289.0
HA 21	1.092E+24	1.914E+24	286.5

HA 22	1.103E+24	1.932E+24	286.5
HA 23	1.116E+24	1.955E+24	286.5

Table 6 Fluence of VVER-1000 RPV BM model steels specimens

Specimen ID.	E>1 MeV [n/m^{-2}]	E>0.5MeV [n/m^{-2}]	Avg. Temp [°C]
A4 112	7.990E+23	1.398E+24	267.1
A4 213	8.224E+23	1.436E+24	267.1
A4 311	8.427E+23	1.470E+24	267.1
A4 313	8.623E+23	1.504E+24	267.1
A4 411	8.836E+23	1.540E+24	267.1
A4 511	9.093E+23	1.584E+24	267.1
B4 112	9.433E+23	1.643E+24	267.1
B4 211	9.904E+23	1.724E+24	267.1
B4 214	1.107E+24	1.940E+24	289.0
B4 311	1.136E+24	1.990E+24	289.0
B4 412	1.161E+24	2.034E+24	289.0
B4 511	1.185E+24	2.076E+24	289.0
C4 111	1.212E+24	2.123E+24	289.0
C4 213	1.244E+24	2.179E+24	289.0
C4 312	1.286E+24	2.253E+24	289.0
C4 313	1.345E+24	2.357E+24	289.0
C4 411	9.600E+23	1.674E+24	271.2
C4 511	9.893E+23	1.727E+24	271.2
D4 113	1.014E+24	1.772E+24	271.2
D4 114	1.038E+24	1.814E+24	271.2
D4 212	1.063E+24	1.858E+24	271.2
D4 312	1.092E+24	1.911E+24	271.2
D4 411	1.131E+24	1.979E+24	271.2
D4 511	1.184E+24	2.074E+24	271.2
E4 113	8.110E+23	1.416E+24	267.1
E4 211	8.267E+23	1.442E+24	267.1
E4 311	8.345E+23	1.454E+24	267.1
E4 313	8.370E+23	1.458E+24	267.1
E4 411	8.358E+23	1.454E+24	267.1
E4 511	8.322E+23	1.447E+24	267.1
F4 114	8.263E+23	1.434E+24	267.1
F4 213	8.183E+23	1.418E+24	267.1
F4 312	1.122E+24	1.962E+24	289.0
F4 214	1.141E+24	1.997E+24	289.0
F4 412	1.151E+24	2.014E+24	289.0
F4 511	1.153E+24	2.019E+24	289.0
G4 111	1.152E+24	2.017E+24	289.0
G4 113	1.147E+24	2.009E+24	289.0
G4 212	1.139E+24	1.995E+24	289.0
G4 313	1.129E+24	1.977E+24	289.0
G4 411	9.904E+23	1.728E+24	271.2
G4 511	1.006E+24	1.756E+24	271.2
H4 111	1.013E+24	1.769E+24	271.2
H4 211	1.015E+24	1.773E+24	271.2

H4 214	1.013E+24	1.771E+24	271.2
H4 313	1.008E+24	1.764E+24	271.2
H4 411	1.002E+24	1.753E+24	271.2
H4 412	9.938E+23	1.740E+24	271.2

Table 7 Fluence of VVER-1000 RPV realistic welds specimens

Specimen ID.	E>1 MeV [n/m-2]	E>0.5MeV [n/m-2]	Avg. Temp °C
KA 11	1.130E+24	1.981E+24	286.5
KA 12	1.146E+24	2.008E+24	286.5
KA 13	1.164E+24	2.039E+24	286.5
KA 21	1.183E+24	2.074E+24	286.5
KA 22	1.205E+24	2.111E+24	286.5
KA 23	1.223E+24	2.144E+24	286.5
LA 11	1.022E+24	1.788E+24	277.2
LA 12	1.032E+24	1.806E+24	277.2
LA 13	1.045E+24	1.829E+24	277.2
LA 21	1.059E+24	1.854E+24	277.2
LA 22	1.075E+24	1.882E+24	277.2
LA 23	1.092E+24	1.911E+24	277.2
MA 11	1.110E+24	1.945E+24	277.2
MA 12	1.131E+24	1.980E+24	277.2
MA 13	1.148E+24	2.012E+24	277.2
MA 21	9.655E+23	1.692E+24	279.3
MA 22	9.872E+23	1.730E+24	279.3
MA 23	1.006E+24	1.763E+24	279.3
NA 11	1.024E+24	1.795E+24	279.3
NA 12	1.043E+24	1.827E+24	279.3
NA 13	1.064E+24	1.865E+24	279.3
NA 21	1.090E+24	1.910E+24	279.3
NA 22	1.123E+24	1.968E+24	279.3
NA 23	1.167E+24	2.045E+24	279.3

Table 8 Fluence of PWR RPV BM model steels specimens

The loading sketch can be found in [10].

Appendix B

Summary of tensile results

Specimen ID	d_0 [mm]	d_u [mm]	S_0 [mm²]	S_u [mm²]	L_o [mm]	L_u [mm]	TE [%]	Z [%]	F_p [kN]	F_m [kN]	YS [MPa]	UTS [MPa]
AA4-1	2.96	2.04	6.88	3.27	15.00	17.75	18.3	52.5	4.032	5.817	585.9	845.3
AA4-2	2.99	2.05	7.02	3.30	15.00	18.25	21.7	53.0	4.253	5.972	605.7	850.5
AA4-3	2.97	2.10	6.93	3.46	15.00	18.00	20.0	50.0	4.274	5.905	616.9	852.3
BA4-1	3.04	1.68	7.26	2.22	15.00	18.50	23.3	69.5	4.067	4.896	560.3	674.5
BA4-2	3.05	1.58	7.31	1.96	15.00	18.50	23.3	73.2	4.164	4.940	569.9	676.1
BA4-3	3.05	1.60	7.31	2.01	15.00	18.25	21.7	72.5	4.109	4.939	562.4	676.0
CA4-1	2.97	1.58	6.93	1.96	15.00	18.00	20.0	71.7	4.040	4.650	583.1	671.2
CA4-2	3.00	1.60	7.07	2.01	15.00	18.75	25.0	71.6	4.100	4.741	580.0	670.7
CA4-3	3.00	1.58	7.07	1.96	15.00	18.00	20.0	72.3	4.075	4.744	576.5	671.1
DA3-1	3.03	1.50	7.21	1.77	15.00	19.30	28.7	75.5	3.867	4.669	536.3	647.5
DA3-2	3.03	1.58	7.21	1.96	15.00	19.20	28.0	72.8	3.842	4.657	532.8	645.8
DA3-3	3.03	1.55	7.21	1.89	15.00	19.00	26.7	73.8	3.852	4.605	534.2	638.6
EA3-1	3.03	1.59	7.21	1.99	15.00	19.15	27.7	72.5	3.383	4.331	469.2	600.6
EA3-2	3.03	1.58	7.21	1.96	15.00	19.45	29.7	72.8	3.388	4.340	469.9	601.9
EA3-3	3.03	1.65	7.21	2.14	15.00	19.30	28.7	70.3	3.408	4.339	472.6	601.7
FA3-1	3.03	1.68	7.21	2.22	15.00	18.78	25.2	69.3	3.780	4.649	524.2	644.7
FA3-2	3.03	1.60	7.21	2.01	15.00	19.40	29.3	72.1	3.776	4.648	523.7	644.6
FA3-3	3.03	1.60	7.21	2.01	15.00	18.55	23.7	72.1	3.782	4.667	524.5	647.2
GA3-1	3.03	1.64	7.21	2.11	15.00	18.40	22.7	70.7	4.103	4.946	569.0	685.9
GA3-2	3.03	1.61	7.21	2.04	15.00	19.00	26.7	71.8	4.110	4.923	570.0	682.7
GA3-3	3.03	1.60	7.21	2.01	15.00	19.35	29.0	72.1	4.116	4.931	570.8	683.8
HA4-1	3.05	1.65	7.31	2.14	15.00	18.50	23.3	70.7	3.527	4.737	482.7	648.4
HA4-2	3.05	1.60	7.31	2.01	15.00	18.75	25.0	72.5	3.558	4.732	487.0	647.7
HA4-3	3.05	1.68	7.31	2.22	15.00	18.50	23.3	69.7	3.604	4.726	493.3	646.9

Table 9 Summary of VVER-1000 RPV BM model steels results from BZN

Specimen ID	d_0 [mm]	d_u [mm]	S_0 [mm²]	S_u [mm²]	L_o [mm]	L_u [mm]	TE [%]	Z [%]	F_p [kN]	F_m [kN]	YS [MPa]	UTS [MPa]
KA3-1	2.97	1.61	6.93	2.04	15.00	18.00	20.0	70.6	4.201	4.873	606.4	703.4
KA3-2	2.94	1.53	6.79	1.84	15.00	18.50	23.3	72.9	4.197	4.785	618.2	704.9
KA3-3	2.94	1.59	6.79	1.99	15.00	18.54	23.6	70.8	4.234	4.791	623.7	705.7
LA3-1	3.00	1.54	7.07	1.86	15.00	18.75	25.0	73.6	4.574	5.173	647.1	731.8
LA3-2	3.00	1.60	7.07	2.01	15.00	18.88	25.9	71.6	4.590	5.182	649.4	733.1
LA3-3	3.01	1.60	7.12	2.01	15.00	18.15	21.0	71.7	4.556	5.205	640.3	731.5
MA3-1	2.95	1.67	6.83	2.19	15.00	18.20	21.3	68.0	3.644	5.211	533.1	762.4
MA3-2	2.94	1.74	6.79	2.38	15.00	18.35	22.3	65.0	3.554	5.156	523.5	759.5
MA3-3	2.94	1.69	6.79	2.24	15.00	18.52	23.5	67.0	3.555	5.171	523.7	761.7

NA3-1	3.00	1.74	7.07	2.38	15.00	18.50	23.3	66.4	4.183	5.143	591.8	727.6
NA3-2	3.03	1.77	7.21	2.46	15.00	18.20	21.3	65.9	4.367	5.228	605.6	725.0
NA3-3	3.01	1.80	7.12	2.54	15.00	17.95	19.7	64.2	4.279	5.165	601.3	725.9

Table 10 Summary of PWR RPV BM model steels results from BZN

Specimen ID	T [ºC]	d_0 [mm]	d_u [mm]	L_o [mm]	L_u [mm]	F_p [kN]	F_m [kN]	F_u [kN]	YS [MPa]	UTS [MPa]	R_u [MPa]	TE [%]	Z [%]
C4_112	24	3,00	1,64	30,07	33,72	4,08	4,80	2,95	577.0	680.0	1398,8	12,13	70,12
C4_113	24	3,01	1,69	30,12	33,85	4,05	4,77	2,96	569.0	671.0	1321,6	12,39	68,48
C4_114	24	3,01	1,70	30,00	34,09	4,45	5,02	3,13	625.0	706.0	1380,8	13,64	68,10
C4_211	300	3,02	1,76	30,13	32,90	3,51	4,04	2,56	490.0	563.0	1054,3	9,20	66,04
C4_212	300	3,00	1,79	30,05	32,74	3,40	4,06	2,67	481.0	574.0	1061,7	8,94	64,40
C4_214	300	3,01	1,81	30,04	32,72	3,61	4,24	2,71	508.0	596.0	1051,9	8,92	63,84
D4_111	24	3,00	1,66	30,16	34,27	4,40	5,04	3,19	623.0	714.0	1475,4	13,62	69,38
D4_112	24	3,01	1,69	30,07	34,07	4,28	5,06	3,06	601.0	711.0	1364,0	13,29	68,48
D4_211	24	3,01	1,81	30,02	33,70	4,51	5,05	3,03	634.0	709.0	1175,9	12,27	63,84
D4_213	300	3,02	1,75	30,12	33,24	3,82	4,30	2,66	533.0	600.0	1105,3	10,37	66,42
D4_214	300	3,02	1,75	30,20	33,06	3,99	4,55	2,89	558.0	635.0	1200,8	9,47	66,42
D4_311	300	3,02	1,81	30,19	32,60	3,82	4,30	2,69	533.0	600.0	1046,0	8,23	64,08
F4_111	24	3,01	1,70	29,83	34,07	4,32	4,88	3,11	607.0	687.0	1370,4	14,20	68,10
F4_112	24	3,02	1,84	30,10	32,63	4,61	5,07	0,42	644.0	708.0	156,1	8,41	62,88
F4_113	24	3,01	1,68	30,10	34,41	4,26	4,86	2,84	599.0	684.0	1279,2	14,33	68,85
F4_211	300	3,01	1,72	29,97	32,70	3,63	4,11	2,60	511.0	577.0	1119,4	9,12	67,35
F4_212	300	3,01	2,57	30,11	33,04	3,65	4,16	2,60	513.0	584.0	501,7	9,74	27,10
F4_311	300	3,01	1,79	30,02	32,78	3,75	4,18	2,76	527.0	587.0	1097,3	9,20	64,64
G4_112	24	3,01	1,74	30,15	34,34	4,54	5,03	3,06	638.0	707.0	1288,8	13,90	66,58
G4_114	24	3,01	1,73	29,69	33,59	4,67	5,14	3,14	656.0	722.0	1334,1	13,14	66,97
G4_211	24	3,01	1,70	30,16	34,49	4,61	5,08	3,05	648.0	713.0	1345,7	14,37	68,10
G4_213	300	3,01	1,84	30,07	32,58	3,83	4,29	2,79	538.0	603.0	1048,2	8,36	62,63
G4_214	300	3,02	1,78	29,91	32,94	4,03	4,49	2,77	563.0	627.0	1114,8	10,11	65,26
G4_311	300	3,00	1,72	30,17	32,78	3,88	4,28	2,68	549.0	605.0	1154,8	8,65	67,13

Table 11 Summary of reference VVER-1000 realistic welds results from UJV

Specimen ID	T [ºC]	d_0 [mm]	d_u [mm]	L_o [mm]	L_u [mm]	F_p [kN]	F_m [kN]	F_u [kN]	YS [MPa]	UTS [MPa]	R_u [MPa]	TE [%]	Z [%]
C4_111	24	3.01	2.11	30.09	33.36	6.40	6.71	4.93	899.7	942.7	1410.2	10.85	50.86
C4_213	24	3.01	1.95	30.11	33.78	6.40	6.73	4.66	898.9	946.1	1558.8	12.20	58.03
C4_312	24	3.02	1.95	30.12	33.73	6.22	6.60	4.55	868.6	921.3	1524.5	11.99	58.31
C4_313	300	3.01	1.99	30.00	32.66	5.07	5.59	3.86	712.3	785.7	1242.6	8.86	56.29
C4_411	300	3.00	1.93	30.02	32.13	5.32	5.68	3.86	752.2	802.9	1319.9	7.03	58.61
C4_511	300	3.00	2.06	30.11	32.22	5.50	5.84	4.19	778.7	825.8	1256.8	7.00	52.85
D4_113	24	3.00	2.39	30.04	33.06	6.15	6.59	5.58	869.6	932.2	1243.9	10.05	36.53
D4_114	24	3.00	1.95	30.00	33.94	6.43	6.78	4.53	909.7	958.5	1515.3	13.13	57.75

D4_212	24	3.01	1.96	30.04	33.56	6.49	6.82	4.72	912	958.1	1563.1	11.73	57.60
D4_312	300	3.01	1.95	30.03	32.46	5.27	5.89	4.22	740.9	827.5	1413.7	8.11	58.03
D4_411	300	3.01	2.12	30.00	32.17	5.50	5.86	4.43	772.3	823.2	1253.7	7.23	50.39
D4_511	300	3.01	2.00	30.00	32.43	5.56	5.96	4.04	781	838.1	1285.3	8.09	55.85
F4_114	24	3.01	1.90	30.02	33.65	6.53	6.77	4.52	918.1	951.2	1595.9	12.08	60.15
F4_213	24	3.01	1.85	30.01	33.63	6.58	6.68	4.42	924.4	939.4	1644.0	12.07	62.22
F4_312	24	3.01	2.00	29.96	33.39	6.20	6.62	4.67	870.8	930.6	1486.4	11.46	55.85
F4_214	300	3.01	1.97	29.94	32.36	5.36	5.67	3.87	753.2	797.3	1270.5	8.09	57.16
F4_412	300	3.01	2.01	29.91	32.38	5.27	5.61	3.83	740.7	789	1208.1	8.26	55.41
F4_511	300	3.00	2.08	29.98	32.46	5.07	5.55	4.02	717.5	785.5	1183.6	8.26	51.93
G4_111	24	3.00	2.05	29.90	33.31	6.69	6.84	5.01	945.7	967.9	1518.0	11.41	53.31
G4_113	24	3.01	1.97	29.92	33.77	6.78	6.95	4.84	952.8	977.4	1586.9	12.87	57.16
G4_212	24	3.01	1.98	29.95	33.42	6.91	7.01	5.16	971	984.6	1675.1	11.58	56.73
G4_313	300	3.01	2.10	29.98	32.30	5.33	5.88	4.69	748.3	825.8	1353.4	7.74	51.33
G4_411	300	3.00	1.98	29.93	32.11	5.90	6.11	4.24	834.3	864	1376.0	7.27	56.44
G4_511	300	3.01	1.99	29.93	32.53	5.81	6.08	4.11	816.5	854.3	1320.4	8.69	56.29

Table 12 Summary of irradiated VVER-1000 realistic welds results from UJV

Specimen ID	T [ºC]	YS [MPa]	UTS [MPa]	UE [%]	TE [%]
A4-111	20	618	695	5.3	12.6
A4-113	20	643	715	5.9	13.9
A4-114	300	580	639	3.0	9.3
A4-211	300	538	601	3.4	9.6
AA3-1	20	574	753	6.9	14.1
AA3-2	20	588	758	7.4	15.2
AA3-3	300	641	795	3.9	10.4
B4-111	20	550	662	5.8	12.2
B4-113	20	549	651	5.6	12.7
B4-114	300	465	577	3.4	10.2
B4-212	300	474	553	3.4	8.6
BA3-1	20	581	661	6.1	17.4
BA3-2	20	581	664	6.0	17.4
BA3-3	300	508	587	3.7	11.5
CA3-1	20	555	635	5.2	15.3
CA3-2	20	563	641	4.9	15.3
CA3-3	300	488	562	3.5	11.6
DA4-1	20	506	620	7.8	18.6
DA4-2	20	506	619	7.7	19.7
DA4-3	300	441	535	6.7	15.1
E4-111	20	611	681	6.7	13.9
E4-112	20	565	671	6.4	13.7
E4-114	300	521	598	3.0	10.2
E4-212	300	474	553	3.4	8.6

EA4-1	20	452	579	9.4	20.8
EA4-2	20	451	578	9.2	20.8
EA4-3	300	393	502	6.0	15.7
FA4-1	20	494	610	7.1	17.6
FA4-2	20	493	610	6.9	18.6
FA4-3	300	443	544	6.4	14.8
GA4-1	20	552	660	6.9	17.5
GA4-2	20	553	661	7.3	17.9
GA4-3	300	480	579	5.5	12.2
H4-112	300	524	589	3.2	10.7
H4-113	20	592	670	7.2	16.2
H4-114	300	528	594	4.8	11.0
H4-311	20	602	681	6.8	14.7
HA3-1	20	480	636	9.7	21.7
HA3-2	20	479	635	9.8	22.3
HA3-3	300	412	560	8.3	15.1

Table 13 Summary of reference VVER-1000 BM model steels and realistic welds results from NRG

Specimen ID	Heat treatment	T [ºC]	YS [MPa]	UTS [MPa]	UE [%]	TE [%]
A4-112		20	884	913	5.5	7.7
A4-213		20	873	911	6.3	13.2
A4-311(HT)	418 °C + 150 hrs	20	635	700	6.2	13.5
A4-313(HT)	418 °C + 150 hrs	20	633	713	5.7	11.4
A4-411(HT)	475 °C + 100 hrs	20	622	688	5.5	11.5
A4-511(HT)	475 °C + 100 hrs	20	633	704	5.4	12.6
AA1-1		20	706	853	4.7	11.9
AA12		20	696	840	5.5	14.0
AA13(HT)	340 °C + 150 hrs	20	667	816	4.6	11.8
AA-2-1(HT)	340 °C + 150 hrs	20	671	824	4.6	12.3
AA2-2(HT)	475 °C + 100 hrs	20	555	746	6.8	16.1
AA2-3(HT)	475 °C + 100 hrs	20	615	761	7.0	16.2
B4-112		20	802	859	5.2	9.6
B4-211		20	786	856	5.7	11.7
B4-214(HT)	418 °C + 150 hrs	20	590	678	5.7	12.4
B4-311(HT)	418 °C + 150 hrs	20	578	660	6.3	15.0
B4-412(HT)	475 °C + 100 hrs	20	554	634	4.9	11.2
B4-511(HT)	475 °C + 100 hrs	20	567	649	6.0	13.5
BA11		20	741	802	6.4	15.3
BA12		20	753	804	6.9	15.4
BA13(HT)	340 °C + 150 hrs	20	729	785	7.3	16.5
BA21(HT)	340 °C + 150 hrs	20	749	800	6.7	15.7
BA2-2(HT)	475 °C + 100 hrs	20	577	658	6.3	17.0

BA2-3(HT)	475 °C + 100 hrs	20	542	661	5.6	17.7
CA1-1		20	840	881	5.6	13.0
CA12		20	832	870	4.6	13.1
CA13(HT)	340 °C + 150 hrs	20	814	861	5.7	13.6
CA21(HT)	340 °C + 150 hrs	20	811	856	5.4	13.6
CA2-2(HT)	475 °C + 100 hrs	20	546	627	5.1	15.2
CA2-3(HT)	475 °C + 100 hrs	20	541	636	5.6	15.2
DA1-1		20	947	999	7.6	14.7
DA12		20	932	988	7.2	15.0
DA1-3(HT)	340 °C + 150 hrs	20	914	971	7.3	15.0
DA2-1(HT)	340 °C + 150 hrs	20	892	956	8.3	17.4
DA2-2(HT)	475 °C + 100 hrs	20	508	617	7.6	19.4
DA2-3(HT)	475 °C + 100 hrs	20	510	621	7.9	20.5
E4-113		20	892	946	6.5	14.1
E4-211		20	904	970	5.7	12.1
E4-311(HT)	418 °C + 150 hrs	20	594	663	7.5	13.6
E4-313(HT)	418 °C + 150 hrs	20	587	671	6.9	14.6
E4-411(HT)	475 °C + 100 hrs	20	580	649	6.8	14.7
E4-511(HT)	475 °C + 100 hrs	20	580	662	5.9	12.8
EA1-1		20	696	786	8.3	16.7
EA1-2		20	694	787	8.0	16.9
EA13(HT)	340 °C + 150 hrs	20	676	773	8.4	16.3
EA21(HT)	340 °C + 150 hrs	20	678	769	8.1	17.1
EA22(HT)	475 °C + 100 hrs	20	454	585	8.6	21.2
EA2-3(HT)	475 °C + 100 hrs	20	457	586	8.9	20.8
FA11		20	775	858	7.9	15.5
FA1-2		20	772	854	7.9	16.5
FA13(HT)	340 °C + 150 hrs	20	763	846	7.9	15.7
FA21(HT)	340 °C + 150 hrs	20	750	830	7.7	17.6
FA22(HT)	475 °C + 100 hrs	20	503	620	7.6	19.7
FA2-3(HT)	475 °C + 100 hrs	20	508	622	7.6	21.7
GA1-1		20	1007	1070	7.2	15.3
GA1-2		20	1015	1066	7.5	14.9
GA1-3(HT)	340 °C + 150 hrs	20	1001	1058	7.9	16.5
GA21(HT)	340 °C + 150 hrs	20	992	1044	7.1	14.8
GA22(HT)	475 °C + 100 hrs	20	555	661	8.6	19.7
GA23(HT)	475 °C + 100 hrs	20	554	656	7.8	18.4
H4-111(HT)	475 °C + 100 hrs	20	611	674	7.0	15.7
H4-211		20	976	1007	0.4	13.7
H4-214		20	949	981	7.0	14.6
H4-313(HT)	418 °C + 150 hrs	20	932	981	6.4	12.3
H4-411(HT)	418 °C + 150 hrs	20	945	984	6.1	12.2
H4-412(HT)	475 °C + 100 hrs	20	594	663	5.9	14.9
HA11		20	931	1025	7.6	14.9
HA12		20	930	1027	8.2	14.6

HA13(HT)	340 °C + 150 hrs	20	918	1030	8.4	15.2
HA21(HT)	340 °C + 150 hrs	20	897	998	7.6	15.1
HA22(HT)	475 °C + 100 hrs	20	479	631	10.2	21.7
HA23(HT)	475 °C + 100 hrs	20	478	632	10.0	22.4

Table 14 Summary of irradiated VVER-1000 BM model steels and realistic welds results from NRG

Specimen ID	T [ºC]	YS [MPa]	UTS [MPa]	UE [%]	TE [%]
KA4-1	20	571	655	5.0	12.6
KA4-2	100	540	621	6.4	16.7
KA4-3	20	571	663	7.9	19.8
LA4-1	20	620	717	7.4	19.4
LA4-2	100	593	686	7.1	16.6
LA4-3	20	613	719	8.0	18.8
MA4-1	20	533	733	7.6	17.7
MA4-2	100	551	669	3.9	14.0
MA4-3	20	612	729	5.2	15.4
NA4-1	20	580	707	7.3	17.3
NA4-2	100	570	687	6.9	15.8
NA4-3	20	607	745	8.2	18.5

Table 15 Summary of reference PWR RPV BM model steels

Specimen ID	Heat treatment	T [ºC]	YS [MPa]	UTS [MPa]	UE [%]	TE [%]
KA1-1		20	719	774	7.3	16.2
KA12		20	723	772	6.1	14.9
KA1-3		100	676	727	6.6	14.6
KA2-1		100	693	743	6.6	14.8
KA2-2(HT)	450 °C + 40 hrs	20	602	677	7.2	17.2
KA2-3(HT)	450 °C + 40 hrs	20	615	685	6.7	16.3
LA1-1		20	761	825	6.9	15.3
LA1-2		20	772	827	8.1	17.1
LA1-3		100	736	799	7.5	15.9
LA2-1		100	718	779	8.0	16.6
LA2-2(HT)	450 °C + 40 hrs	20	654	739	7.5	16.9
LA2-3(HT)	450 °C + 40 hrs	20	654	741	7.3	16.5
MA1-1		20	852	959	4.5	12.5
MA1-2		20	832	962	4.9	12.8
MA1-3		100	772	904	3.7	10.4
MA2-1		100	844	974	4.0	11.1
MA2-2(HT)	450 °C + 40 hrs	20	615	748	5.2	14.2

MA2-3(HT)	450 °C + 40 hrs	20	594	737	6.1	15.0
NA1-1		20	951	1054	6.5	14.2
NA1-2		20	986	1047	6.7	15.0
NA1-3		100	926	1005	5.7	12.3
NA2-1		100	917	992	6.6	14.0
NA2-2(HT)	450 °C + 40 hrs	20	621	740	7.9	18.3
NA2-3(HT)	450 °C + 40 hrs	20	625	744	7.8	17.5

Table 16 Summary of irradiated PWR RPV BM model steels